Solubilisation and cytotoxicity of albendazole encapsulated in cucurbit[*n*]uril

Yunjie Zhao,[a] Damian P. Buck,[a] David L. Morris,[b] Mohammad H. Pourgholami,*[b] Anthony I. Day*[a] and J. Grant Collins*[a]

Received 7th August 2008, Accepted 13th October 2008
First published as an Advance Article on the web 6th November 2008
DOI: 10.1039/b813759e

The aqueous solubilities of albendazole encapsulated in cucurbit[6, 7 and 8]urils (Q[6], Q[7] and Q[8]) have been determined by ^{1}H NMR spectroscopy, and the effect of encapsulation on their cytotoxicities evaluated. Encapsulation in Q[6] and Q[7] increased the aqueous solubility of albendazole by 2 000-fold, from 3 μM to 6 mM at pH 6.6, while Q[8]-encapsulation increased the solubility to over 2 mM. Encapsulation in Q[7] and Q[8] induced significant upfield shifts for the albendazole propyl and benzimidazole resonances, compared to those observed for Q[6]-binding and what would normally be expected for the respective functional groups. The upfield shifts indicate that the albendazole propyl and benzimidazole protons are located within the Q[7] and Q[8] cavity upon encapsulation. Alternatively, encapsulation in Q[6] only induced a large upfield shift for the albendazole carbamate methyl resonance, indicating that the drug associates with Q[6] at its portals, with only the carbamate group within the cavity. Simple molecular models based on the observed relative changes in chemical shift could be constructed that were consistent with the conclusions from the NMR experiments. Cytotoxicity assays against human colorectal cells (HT-29), human ovarian cancer cells (1A9) and the human T-cell acute lymphoblastic leukaemia cells (CEM) indicated that encapsulation in Q[7] did not significantly reduce the *in vitro* anti-cancer activity of albendazole.

Introduction

Albendazole (ABZ), methyl 5-propylthio-1*H*-benzimidazole-2-yl carbamate (see Fig. 1), is known as a broad spectrum anti-parasitic primarily used in the treatment of worms such as hookworms, whipworms and roundworms.[1–3] More recently, ABZ has been shown to exhibit significant anti-tumour activity.[4–7] ABZ is thought to bind to β-tubulin, a major target of drug molecules, and inhibit microtubule polymerisation;[8,9] however, other mechanisms of action have also been suggested, *e.g.* disruption of glucose uptake leading to ATP depletion.[10] Pourgholami *et al.* have shown that ABZ inhibits hepatocellular carcinoma cell proliferation under both *in vitro* and *in vivo* conditions,[4] while over the last few years, ABZ has been shown to exhibit significant activity against a number of other cancer cell lines, *e.g.* colorectal and ovarian cancers, and leukaemia.[5–7] Additionally, potent inhibitory effects of the drug on vascular endothelial growth factor (VEGF) and ascites has been described.[6]

While ABZ has potent anti-proliferative activity, its clinical application as an anti-cancer agent is limited by its aqueous solubility. In a recent study of 15 poorly soluble drugs, Bergström *et al.* measured the intrinsic aqueous solubility of albendazole to be 0.983 ± 0.112 μM.[11] There are a variety of possible strategies to increase the solubility of ABZ, and in this study we have examined the effect of encapsulating ABZ in macrocyclic molecules called cucurbiturils. Cucurbit[*n*]uril, compounds best described as open ended barrels (see Fig. 1) made from the condensation of glycoluril and formaldehyde, are capable of binding small molecules under a variety of conditions.[12–21] Importantly a range of cavity sizes are available (Q[5]–Q[10], portal openings of ~2.4–11.0 Å including the van der Waals radii), which enables a thorough examination of Q[*n*] as a suitable molecular carrier. For Q[7] the portal diameter is 5.4 Å, the cavity diameter 7.3 Å, with a height of 9.1 Å, whereas

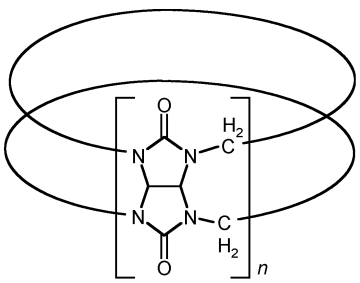

B

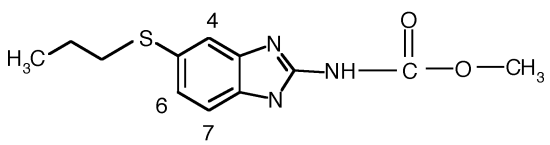

A

Fig. 1 Structure and atom numbering of albendazole (A) and structure of cucurbit[*n*]uril (B).

[a]*School of Physical, Environmental and Mathematical Sciences, University College, University of New South Wales, Australian Defence Force Academy, Northcott Drive, Campbell, ACT 2600, Australia. E-mail: a.day@adfa.edu.au; g.collins@adfa.edu.au; Fax: (02) 6268 8017*
[b]*University of New South Wales Department of Surgery, St. George Hospital (SESIAHS), Sydney, NSW, 2217, Australia. E-mail: mh.pourgholami@unsw.edu.au*

Q[6] and Q[8] have the same height as Q[7] but different portal (3.9 and 6.9 Å respectively) and cavity diameters (5.8 and 8.8 Å respectively).[17]

The binding of molecular guests by Q[*n*] in aqueous systems is facilitated by the hydrophobic effect and van der Waals forces associated with the cavity, while ion–dipole and hydrogen bonding interactions can occur at the portals.[17] The inner cavity of Q[*n*] should be able to accommodate part of the propylthiobenzimidazole section of the drug, thereby significantly increasing the aqueous solubility. The NMR results of this study demonstrate that encapsulation by cucurbit[6,7,8]uril does increase the solubility of albendazole to mM levels without significantly affecting the *in vitro* cytotoxicity against a range of cancer cell lines.

Experimental

Materials

ABZ was purchased from the Sigma Chemical Company, while D_2O was obtained from Cambridge Isotope Laboratories. Q[6], Q[7] and Q[8] were synthesised as previously described.[12,13] All solvents were used as provided and aqueous solutions were made using Milli-Q water, coming from a Millipore four-stage water purification unit.

Cucurbit[*n*]uril titrations of ABZ

Q[7] was dissolved in D_2O to a specific concentration and then mixed with known weights of ABZ, whereas, Q[6] and Q[8], which are sparingly soluble in water, were added to albendazole and D_2O in solid form. All samples were shaken using a vortex shaker, sonicated and then left standing overnight before analysis by NMR spectroscopy.

Albendazole aqueous solubility

An excess of the drug was added to 150 mL of water at either pH 3.0 or 6.6, the suspension sonicated for 90 minutes and then left standing overnight at 20 °C. The suspension was then filtered through a 0.5 μm PETE syringe filter, freeze-dried and then redissolved in 20 mL of methanol. The concentration of albendazole was determined from the absorption at 295.7 nm against a standard curve.

NMR spectroscopy

NMR spectra were obtained on a Varian Unity*plus-400* spectrometer operating at 400 MHz for the ^{1}H nuclei. One-dimensional ^{1}H NMR spectra were recorded over a spectral width of 5000 Hz using 256 transients. All spectra were referenced to DSS (0 ppm) at 25 °C, using the residual HDO resonance at 4.78 ppm as an internal reference signal. ABZ concentrations in solution were measured by comparing the integrals of the albendazole ^{1}H peaks with those of two known concentrations of ethanol, typically 2 mM and 6 mM. The results were corrected for the different spin-lattice (T1) relaxation times between the ethanol and ABZ protons. T1 times were determined using the standard 180°-τ-90° pulse sequence. The concentration ratio of ABZ to cucurbituril was determined by comparing the ^{1}H resonance integrals of ABZ with those of the Qs.

Phase-sensitive NOESY spectra were acquired using 2048 data points in t_2 for 256 t_1 values with a pulse repetition delay of 1.7 s for mixing times of 350 ms. Saturation transfer experiments were carried out using a 1:1:1 molar ratio mixture of ABZ:Q[7]:Q[8] with each component 1 mM in D_2O. Q[8] was initially mixed with ABZ, since the presence of Q[7] prevented Q[8] solvation. Only after the Q[8] and ABZ concentrations were confirmed to be 1 mM was Q[7] added as a solid. The benzimidazole aromatic proton singlet resonance of ABZ encapsulated by Q[8] was selectively irradiated (saturated). The spectrum with the Q[8] peak saturation was subtracted from that of the control spectrum (where the irradiation frequency was in a region of the spectrum that contained no resonances) to determine the extent of saturation transferred from the benzimidazole singlet of ABZ bound by Q[8] to the equivalent signal of that bound by Q[7]. The number of scans for each spectrum was 1024, with a pulse repetition delay of 15 seconds. The control and saturation pulses were interleaved.

Molecular modelling

Molecular modelling was carried out using HyperChem.[22] The molecular mechanics (Amber99) forcefield was used for ABZ, and was minimised to a root-mean-square gradient of 0.002 kJ (A mol)$^{-1}$. Cucurbit[*n*]uril models were optimised separately using the MM+ forcefield, as the stretch-bend cross term was required to accurately reflect the rigidity conferred by the five and eight membered rings. Subsequent optimisations treated the Q[*n*] as rigid and were performed using Amber99 with Q[*n*] point charges based on a previous semi-empirical calculation (AM1). The Amber forcefield, which does not have the stretch-bend cross term, was used to more closely reflect the van der Waals radii within the confined spaces of the Q[*n*] than is possible with MM+.

Preparation of ABZ-Q[7] complexes for *in vitro* testing

A typical preparation involved mixing solid ABZ (4.1 mg, 15 μmol) and solid Q[7] (21.5 mg, 15 μmol) in H_2O (1.5 mL). Using a vortex shaker the mixture was homogenised, sonicated for 1.5 h and then left to stand overnight at 20 °C. Filtration through a 0.5 μm PETE syringe filter gave clear solutions of ABZ-Q[7] complex. Solid product was obtained by lyophilisation. The mole ratio of ABZ:Q[7] was determined by ^{1}H NMR and microanalysis. Both methods were found to be consistently in agreement with mole ratios between 0.6–0.7:1 respectively. The exact mole ratio for each preparation was determined before use. Samples dissolved in D_2O were compared by peak area integrals against additions of 10 μL of standardised ethanol (125 mM) in D_2O, using ^{1}H NMR. The carbon to sulfur ratio found in microanalysis samples, dried at 50 °C in *vacuo* (0.5 mm Hg), was used to calculate the ABZ:Q[7] mole ratio. A microanalysis for a 0.6:1 ratio sample with 14 H_2O and 1 HCl was, found: C 36.63, H 4.62, N 26.20, S 1.19, Cl 2.18. $C_{49.2}H_{79}N_{29.8}O_{29.2}S_{0.6}Cl$ requires C 36.69, H 5.01, N 25.91, S 1.19, Cl 2.20%.

The concentrations of ABZ for *in vitro* testing were calculated and prepared in saline solutions in accordance with the determined ABZ-Q[7] ratios of the above lyophilised preparations.

Cell proliferation assay

The human colorectal and ovarian cancer cells HT-29 and 1A9, respectively, were obtained from ATCC (USA) and the human T-cell acute lymphoblastic leukaemia cells (CEM) were kindly provided by Prof. Maria Kavallaris (Children's Cancer Institute Australia for Medical Research). Cells were maintained in RPMI-1640 medium supplemented with 10% fetal bovine serum and were grown in a humidified incubator at 37 °C under a 5% CO_2/95% air atmosphere. Anti-proliferative effects of Q[7]-encapsulated ABZ on these cells was determined by the MTT (3-(4,5-dimethylthiazol-2-yl)-2,5-diphenyl tetrazolium bromide) assay.[23] Cells seeded in 96-well plates were treated with various concentrations of ABZ-Q[7] (0, 0.1, 1 or 10 μM in ABZ) for 72 h. At the end of the incubation period, 0.5 mg/ml of MTT was added to each well and plates were incubated for a further 4 h for colour development. Following this, cells were solubilised by the addition of 100 μl of dimethyl sulfoxide to each well. The absorbance was read at 562 nm on a plate reader. Each drug concentration was in a replicate of 8 and each experiment was performed at least twice.

Results

Cucurbituril encapsulation of albendazole, ABZ

Fig. 2 shows the ^{1}H NMR spectra of ABZ with added Q[6], Q[7] and Q[8] at pH 3.0, the pH obtained upon mixing ABZ with Q[*n*]. Importantly, and as evidenced by the observation of strong resonances that can be assigned to the drug, addition of the Q[*n*] solubilised the ABZ. In control experiments, the aqueous solubility of ABZ at pH 6.6 was found to be 3 (±0.5) μM, consistent with the reported aqueous solubility of 1 μM,[11] and 17 (±1) μM at pH 3.0. The maximum solubility obtainable with Q[6,7,8] is summarised in Table 1. For the only relatively aqueous soluble cucurbituril, Q[7], it was noted that the maximum solubility that could be obtained within 24 hours was only 2.2 mM if the ABZ was initially added to a Q[7] solution at pH 6.6. However, no decrease in ABZ solubility from 6 mM was observed when the pH of an ABZ-Q[7] sample prepared at pH 3.0 was raised to 6.6.

As observed in Fig. 2, only one set of ABZ resonances is observed in the spectrum of the drug with added Q[*n*]. However, there is considerable difference in the chemical shift of the resonances from ABZ when solubilised by Q[6] compared to that with Q[7] and Q[8] (see Table 2). The chemical shifts observed for the aromatic and propyl protons of ABZ associated with Q[6]

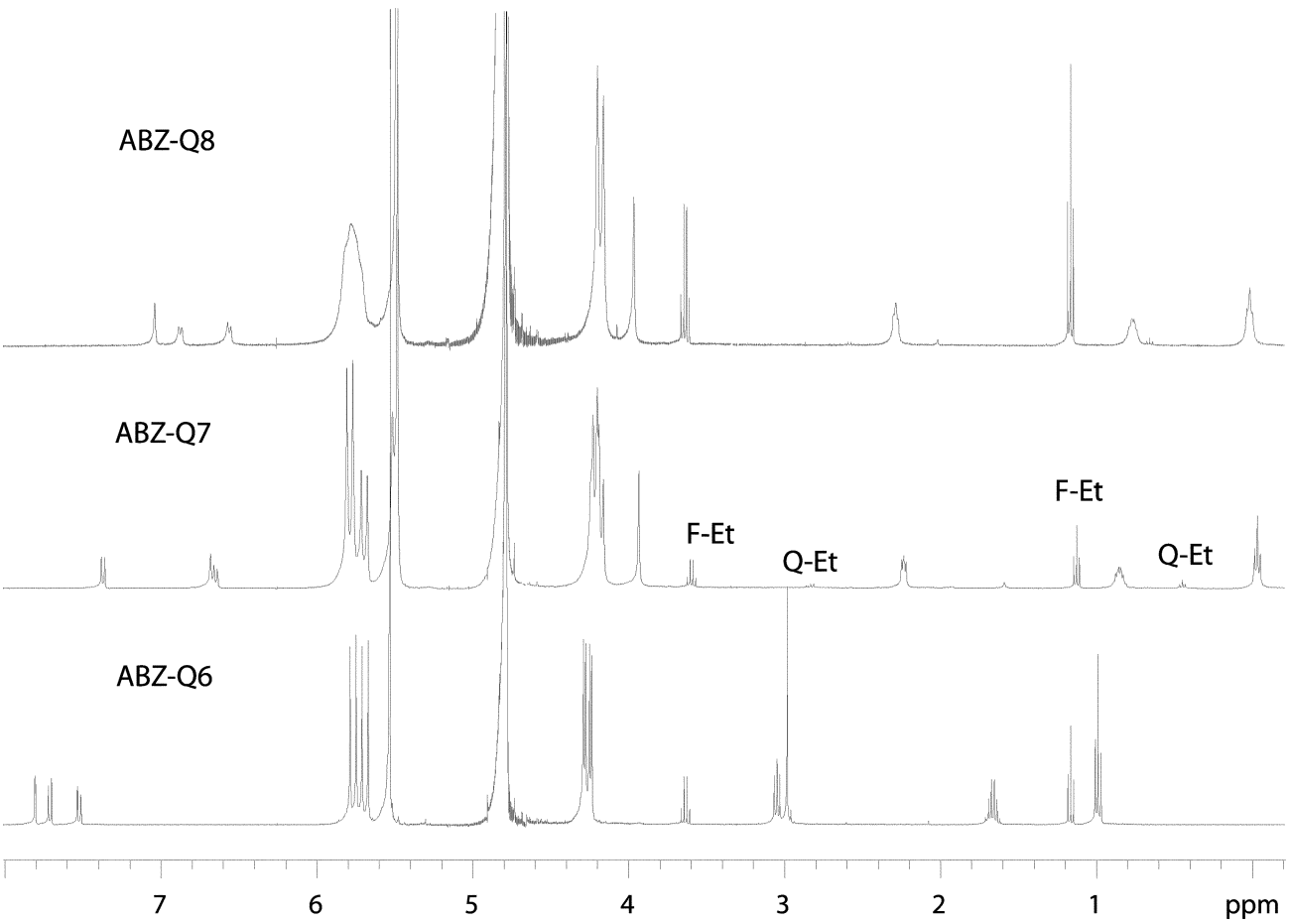

Fig. 2 ^{1}H NMR spectra of albendazole in D_2O with Q[6], Q[7] and Q[8] containing 2.05 mM added ethanol at 25 °C, at a drug to cucurbit[*n*]uril mixed ratio of 1:1. F-Et denotes free ethanol, while Q-ET indicates ethanol bound in the cucurbit[7]uril.

Table 1 Maximum solubility (mM) of albendazole encapsulated in cucurbit[*n*]uril in D_2O at pH 3.0 at 25 °C

Cucurbit[*n*]uril	ABZ:Q Mixed Ratio[a] (MR)	ABZ:Q Solution Ratio[b]	ABZ Solubility/mM[c]
6	1	0.92	5.8
6	2	0.90	5.6
7	0.5	0.5	6.2
7	1	0.71	5.6
7	2	0.76	7.1
8	0.5	0.79	2.2
8	1	0.9	2.7

[a] Solid ABZ (2.7 mg) and the appropriate proportion of Q[*n*] are combined with D_2O (1.0 mL) at 20 °C, shaken, sonicated and set aside for 20 h. [b] Resultant mixtures were filtered and the ratios determined by ^{1}H NMR at 25 °C using standardised EtOH/D_2O solutions. [c] Concentrations of ABZ were determined by the same method as in footnote b.

Table 2 Chemical shifts of the non-exchangeable proton resonances of albendazole encapsulated in Q[6,7,8]. The aromatic resonances of albendazole were assigned by analysis of their coupling pattern, with long range coupling observed between H4 and H6 in the Q[6]- and Q[7]-encapsulated samples. For Q[8]-encapsulated albendazole, the H6 was identified in NOE experiments due to its closer proximity to H4

	Chemical shift (ppm)		
Proton	ABZ-Q[6]	ABZ-Q[7]	ABZ-Q[8]
S-propyl			
CH_3	0.99	–0.03	0.02
CH_2	1.67	0.85	0.77
CH_2	3.05	2.23	2.29
Aromatic			
H4	7.81	6.68	7.04
H6	7.52	6.65	6.88
H7	7.71	7.37	6.56
Carbamate			
CH_3	2.98	3.93	3.97

are similar to the expected values for these types of functional groups, whereas, the carbamate methyl resonance (2.98 ppm) is approximately 1 ppm upfield from what would be expected. Furthermore, with the exception of the carbamate methyl group, all the ABZ resonances are significantly downfield in the spectrum with added Q[6], compared to the corresponding peaks in the spectra with Q[7] and Q[8]. It has now been established that upfield shifts are expected for resonances from guest protons that are located within the cucurbituril cavity, with the largest shifts for protons that are positioned towards the centre of the cavity.[12,19,24] Whereas, small downfield shifts are observed for resonances from guest protons located close to but outside of the cucurbituril portal.

Based on the observed upfield shifts, it is concluded that the ABZ propyl and aromatic protons are located within the Q[7] or Q[8] cavity. Alternatively, as the carbamate methyl resonance has a chemical shift similar to what would be expected for this functional group (approximately 4 ppm), it is concluded that the carbamate methyl is positioned outside of the cucurbituril cavity. As the aromatic resonances from ABZ exhibit different changes in chemical shift upon Q[8]-binding compared to Q[7]-binding (see Table 2), it is also concluded that the drug is positioned within the cavities of Q[7] and Q[8] in slightly different orientations. Based on the observed chemical shifts for the ABZ protons with Q[6] it is concluded that the drug predominantly associates with Q[6] at its portals, with only the carbamate group positioned within the cavity.

The large upfield shifts of the propyl methyl and aromatic resonances in the spectra of ABZ with Q[7] and Q[8] indicate that both these groups must be positioned deep within the cucurbituril cavity. This could occur if the propyl chain folds back into the cavity that also contains the aromatic ring system. The larger cavity volume of Q[8], compared to Q[7], would then allow for different binding orientations. Alternatively, the upfield shifts for both the propyl methyl and aromatic resonances could possibly occur if ABZ and cucurbituril bind in a 1:2 stoichiometry. For Q[7], which is soluble at 10 mM, the ratio of soluble ABZ (determined by NMR) to Q[7] was 0.71 when the drug and Q[7] were initially mixed in ratios (MR) of 1 (see Table 1). Alternatively, for a MR = 0.5 sample, the soluble ABZ -Q[7] complex had an ABZ to Q[7] ratio of 0.5. This suggests that Q[7] can bind albendazole with a 1:2 ABZ:Q[7] stoichiometry. This proposal is supported by the small, but significant (up to 0.07 ppm), downfield shift observed for the albendazole aromatic resonances as more Q[7] is added to a MR = 1 sample. However, as the 1:2 binding is presumably not significantly more stable than 1:1 binding, an equilibrium exists between 1:1 and 1:2 stoichiometries when ABZ and Q[7] are initially mixed in equal molar amounts. This equilibrium then results in a soluble drug to Q[7] ratio <1 even though the mixed ratio MR is ≥1. As only one set of ABZ resonances was observed in all spectra of the drug encapsulated in Q[7], the rate of exchange between 1:2 and 1:1 binding forms must be fast on the NMR time scale.

Rate of dissociation of ABZ from Q[7]

As the chemical shifts of the aromatic resonances of the Q[7]- and Q[8]-bound drug are different, the relative cucurbituril binding affinity can be determined from a competitive binding experiment. Fig. 3 shows the ^{1}H NMR spectrum of a mixture of ABZ, Q[7] and Q[8] where all components are 1 mM in concentration. The resonances from the Q[7]-bound drug are approximately two-fold larger (comparison of integrals) than the corresponding Q[8]-bound resonances, indicating that ABZ has a slightly higher affinity for Q[7] than Q[8].

As separate resonances can be seen for the aromatic protons of the Q[7]- and Q[8]-bound ABZ, the rate of exchange between the two cucurbiturils must be slow on the NMR time scale. Saturation transfer experiments can be used to obtain an estimate of the rate of exchange of the drug between the two cucurbiturils. In an NMR saturation transfer experiment, a resonance from one of the bound forms is selectively radiated, and the saturation is transferred to

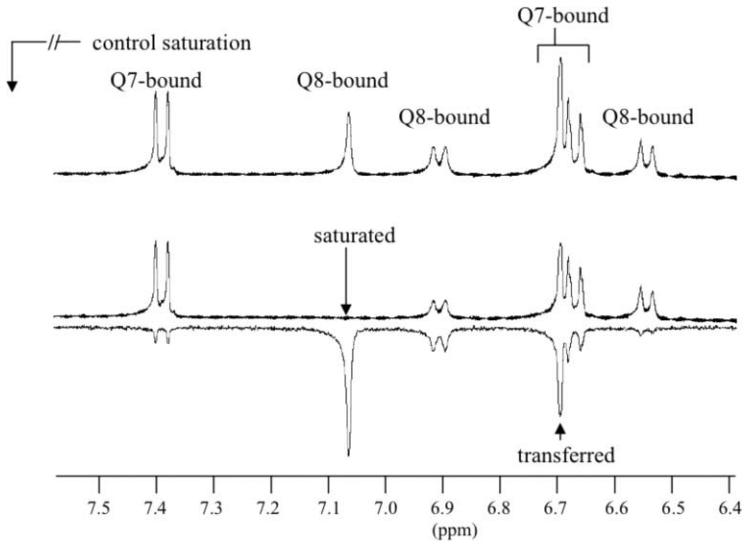

Fig. 3 ^{1}H NMR saturation transfer experiment of a 1 mM solution of a 1:1:1 concentration mixture of albendazole:Q[7]:Q[8] in D_2O at 25 °C. The top spectrum shows the standard ^{1}H NMR spectrum of the mixture, the middle spectrum has the Q[8]-bound H4 selectively irradiated and the lower spectrum is the difference spectrum between the control and Q[8]-H4 irradiated spectra.

the corresponding resonance of the other bound form if the rate of exchange is of a similar order of time as the spin-lattice relaxation times (2.5 s for the H4 aromatic proton). The saturation transfer experiment, see Fig. 3, implied a rate of transfer from Q[8] to Q[7] of approximately one per three seconds.

Molecular modelling

Molecular modelling was utilised to support conclusions drawn from the NMR experiments of the binding of ABZ to Q[6], Q[7] and Q[8]. No intermolecular NOE cross-peaks were observed in NOESY spectra of the encapsulated drug. The lack of intermolecular NOE cross-peaks is due to the cucurbit[*n*]uril protons being exo-cyclic, and thereby at a significant distance from the ABZ protons, coupled with the relative flexibility of the position of the drug within the cucurbit[*n*]uril cavity. Consequently, the starting positions for the energy minimisations were based on the relative chemical shift of the encapsulated ABZ resonances. Models for both 1:1 and 1:2 ABZ to Q[*n*] binding modes were examined.

Models clearly indicate that the cucurbituril cavity is not deep enough to encapsulate both the propyl and aromatic groups if the thioether arm extends away from the benzimidazole ring. This suggests two possible 1:1 binding modes: (A) where the thioether arm is extended and the cucurbituril "shuttles" backwards and forwards over the benzimidazole and propyl groups, or (B) the propyl-arm "folds" back into the cucurbituril cavity. The methyl group from the propyl-arm shifts further upfield than either of the methylene protons in the Q[7]- and Q[8]-bound forms, compared to their respective chemical shifts in the spectrum of the drug with added Q[6] where the propyl group is located outside of the cavity. This strongly suggests that the propyl-arm folds back into the cavity, with the methyl group being positioned towards the centre of the cucurbituril cavity.

Energy minimised 1:1 binding models for Q[7] and Q[8] are shown in Fig. 4. The Q[7] and Q[8] binding models demonstrate

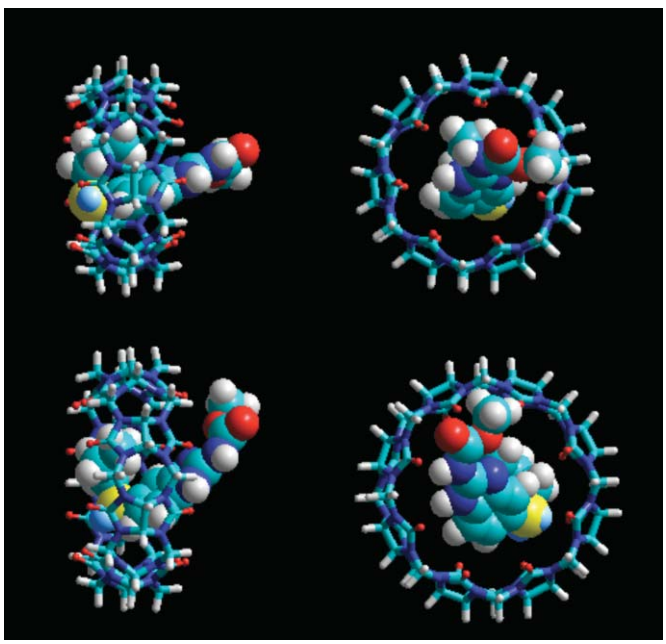

Fig. 4 HyperChem models, equatorial (left) and transverse (right) views, of albendazole encapsulated by Q[7] (top) and Q[8] (bottom). The cucurbiturils are rendered in tubes rather than overlapping spheres for clarity. Electron pairs on divalent sulfur atoms are treated explicitly by the Amber forcefield, and are depicted in light blue.

that it is energetically and sterically reasonable for most of the benzimidazole ring system and the propyl group to be simultaneously positioned within the cavity, in agreement with the NMR results. The larger cavity of Q[8] allows more room for the propyl-arm to fold, and thereby allows the ABZ to bind in a slightly different orientation compared with Q[7]. For example, the aromatic H7 proton is located deeper within the Q[8] cavity than in Q[7], consistent with the NMR results where the H7 shifted

upfield to a greater extent for Q[8]-encapsulation compared to that with Q[7]. The folding back of the propyl chain withdraws it from water, leaving the polar carbamate group positioned at the cucurbituril portal where it can be solvated. The cavity of Q[6] is not large enough to allow a similar binding mode to Q[7] and Q[8].

Energy-minimised molecular models indicate that ABZ can be encapsulated by Q[7] and Q[8] with a 1:2 binding ratio. However, it was not possible (due to the repulsion of the two cucurbiturils) to obtain a model where both the propyl group and the benzimidazole H4, H6 and H7 protons are simultaneously located within a cucurbituril cavity. Fig. 5 shows a representative 1:2 binding model with Q[7]. In this model, one Q[7] is positioned over the methyl group of the propyl-arm with the second Q[7] positioned primarily over the imidazole ring. In this static model, the aromatic protons are located outside of the Q[7] cavity, and hence, the aromatic resonances would be expected to be shifted downfield relative to the corresponding resonances in the Q[6]-encapsulated case. However, as previously noted, only small downfield shifts were observed for the aromatic resonances of a 1:1 mixed ratio ABZ-Q[7] sample (solution ratio 0.7:1) when further Q[7] was added to a final mixed ratio of 1:3. Given the large upfield shifts observed for both the propyl and aromatic protons for the Q[7]- and Q[8]-encapsulated samples, compared to the Q[6] case, it is concluded that the 1:2 binding mode is not the dominant form compared to the 1:1 stoichiometry.

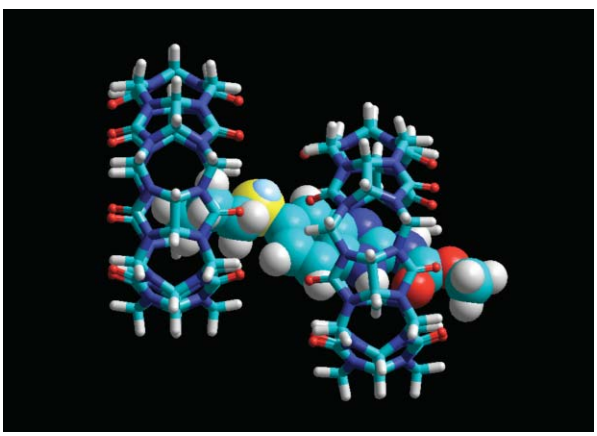

Fig. 5 A HyperChem model of albendazole encapsulated by two Q[7]. The cucurbituril is rendered in tubes rather than overlapping spheres for clarity. Electron pairs on divalent sulfur atoms are treated explicitly by the Amber forcefield, and are depicted in light blue.

In vitro cytotoxicity

To determine the effect of encapsulation on the cytotoxicity of ABZ, the Q[7]-bound drug was tested against human colorectal cells (HT-29), human ovarian cancer cells (1A9) and the human T-cell acute lymphoblastic leukaemia cells (CEM). The results (see Fig. 6) show that the Q[7]-encapsulated drug is effective in inhibiting proliferation of this diverse set of cells. In all cases, the activity of the Q[7]-encapsulated ABZ is slightly less than that of the free drug dissolved in ethanol; however, the IC_{50} (the concentration of drug required to inhibit cell growth by 50%) values for each cell line remain <1 μM.

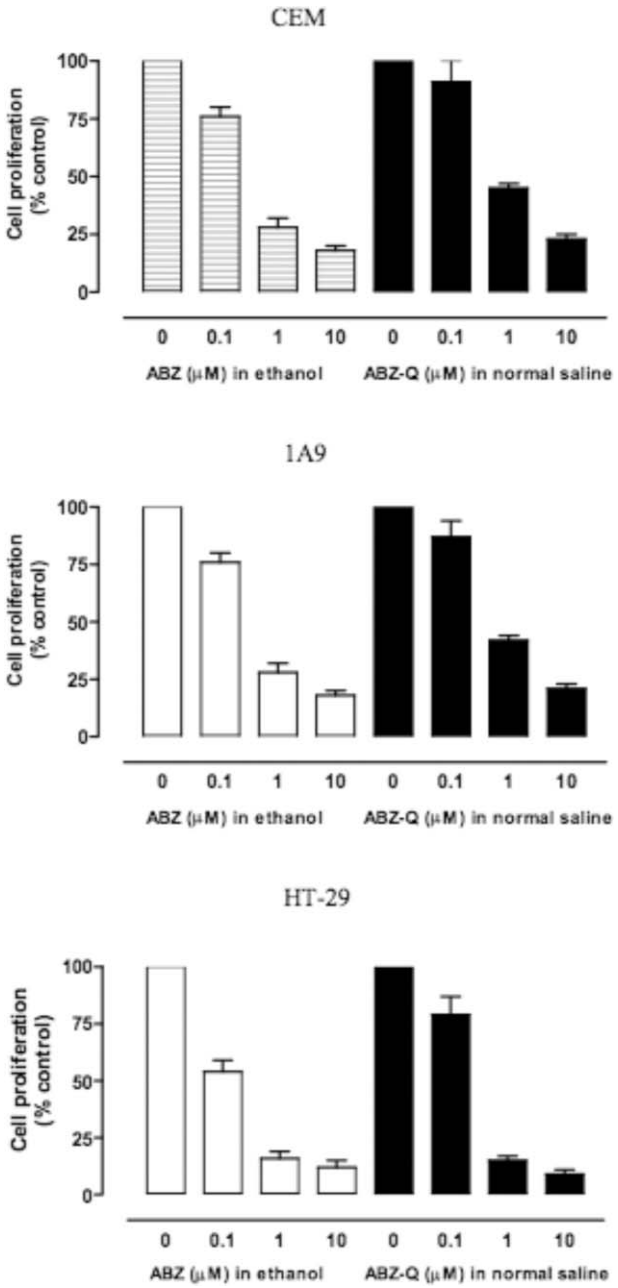

Fig. 6 Effect of ABZ dissolved in ethanol and ABZ encapsulated in Q[7] (concentrations based on ABZ) dissolved in normal saline on the proliferation of human T-cell acute lymphoblastic leukaemia cells (CEM), ovarian cancer cells (1A9) and colorectal cells (HT-29) in cell culture medium. Plates containing the treated cells were left at standard conditions in a 37 °C incubator for 72 h. Effect of the 2 preparations on cell proliferation was assessed using a MTT assay. Results (mean ± SD) are expressed as % of control.

Discussion

Like many other potential anti-cancer agents, the clinical application of ABZ is limited to some degree by its lack of solubility in water.[25–27] Encapsulation in Q[6] and Q[7] increases the water solubility of the drug by 300 to 400-fold at pH 3 and 2 000-fold at pH 6.6. However, it was noted that if ABZ is directly added to a Q[7] solution at pH 6.6, the maximum solubility achievable within

24 hours was only 2.2 mM. This suggests that equilibrium is not reached within 24 hours when ABZ is added to a Q[7] solution at pH 6.6. The maximum solubility of 6 mM is only achievable within 24 hours at pH 3.0 or at pH 6.6 if the ABZ-Q[7] complex is initially prepared at pH 3.0. In a recent paper, Saleh *et al.* demonstrated that the pK_a of a Q[7] encapsulated drug can increase by 4 pK_a units compared to the free drug.[28] As the pK_a values for ABZ are 2.80 and 10.26,[29] the drug would be partially protonated in aqueous solution at pH 3.0. However, based on the results of Saleh *et al.*,[28] ABZ would be fully protonated when encapsulated at pH 3 and would remain protonated when the pH is raised to 6.6, thereby maintaining the solubility achieved at the lower pH.

Encapsulation in Q[8] also increased the aqueous solubility of ABZ, but to a significantly smaller degree. It is probable that the lower solubility obtained with Q[8] simply reflects the lower solubility of the encapsulated complex, rather than a significantly lower affinity for the drug. Given the sparing solubility of Q[8] and mode of binding for Q[6], it is proposed that formulation with Q[7] would also be easier and could impart greater protective benefits. *In vitro* cytotoxicity assays demonstrated that ABZ encapsulated in Q[7] was active against a range of human cancer cell lines at 1 μM concentrations. However, it was noted that the Q[7]-encapsulated ABZ was slightly less active than the free ABZ dissolved in ethanol in each of the three cell lines. The observed cytotoxicity is a function of both the rate of release of the drug from the cucurbituril and the amount of free drug that is available to interact with the bio-receptors. Although the strong binding affinity of ABZ for Q[7] indicates that the drug will predominantly be encapsulated, the saturation transfer experiments demonstrated that the drug could dissociate from the cucurbituril within seconds and bind to a receptor if the affinity is at least comparable to that with Q[7]. Consequently, the reduction of activity observed for the Q[7]-bound ABZ must be due to the high proportion of drug that is encapsulated, and not available for binding to bio-receptors, at any time point. As ABZ is active at concentrations below its aqueous solubility, it is proposed that encapsulation within cucurbituril will allow it to be transported through the body at significantly higher concentrations, and subsequently be released into cells at cytotoxic concentrations. Initial toxicity studies have indicated that the *in vivo* tolerance, based on a 10% weight loss, of Q[7] when administered intravenously in mice is 200 mg/kg.[30] This is far in excess of the amount of Q[7] required to deliver ABZ.

Encapsulation in Q[7] may also protect ABZ from degradation into less cytotoxic or inactive species, such as the thioether oxidation products. We have previously demonstrated that encapsulation of multinuclear platinum complexes in cucurbiturils can protect the platinum centres from reaction with thiol containing blood proteins.[21] The major known metabolites of albendazole are the sulfoxide and sulfone derivatives.[31] Upon oral administration, ABZ is rapidly metabolised in the liver to the sulfoxide and sulfone derivatives resulting in extremely low to undetectable ABZ levels.[31] The sulfoxide is approximately 20-fold less cytotoxic than ABZ, while the sulfone derivative is inactive.[5] From the molecular modelling, and the previous results using multinuclear platinum drugs,[21] it is reasonable to expect that encapsulation would provide significant protection against oxidation for the ABZ sulfur atom.

In conclusion, encapsulation of ABZ may provide a formulation method to solubilise the drug for clinical application.

References

1 D. L. Morris, P. W. Dykes, B. Dickson, S. E. Marriner, J. A. Bogan and F. G. O. Burrows, *Br. Med. J.*, 1983, **286**, 103.
2 K. Hanjeet and R. G. Mathias, *Acta. Trop.*, 1991, **50**, 111.
3 W. T. James and T. W. Leslie, Drugs used in the chemotherapy of helminthiasis, in *The pharmacological basis of therapeutics by Goodman and Gilman*, 9th edition. McGraw Hill, New York.
4 M. H. Pourgholami, L. Woon, R. Almajd, J. Akhter, P. Bowery and D. L. Morris, *Cancer Lett.*, 2001, **165**, 43.
5 M. H. Pourgholami, J. Akhter, L. Wang, Y. Lu and D. L. Morris, *Cancer Chemother. Pharmacol.*, 2005, **55**, 425.
6 M. H. Pourgholami, Z. Yan Cai, Y. Lu, L. Wang and D. L. Morris, *Clin. Cancer Res.*, 2006, **12**, 1928.
7 A. Khalilzadeh, K. T. Wangoo, D. L. Morris and M. H. Pourgholami, *Biochem. Pharmacol.*, 2007, **74**, 407.
8 P. A. Friedman and E. G. Platzer, *Biochem. Biophys. Acta*, 1978, **544**, 605.
9 C. M. Ireland, K. Gull, W. E. Gutteridge and C. I. Pogson, *Biochem. Pharmacol.*, 1979, **28**, 2680.
10 E. Lacey, *Int. J. Parasitol.*, 1988, **18**, 885.
11 C. A. S. Bergstrom, C. M. Wassvik, K. Johansson and I. Hubatsch, *J. Med. Chem.*, 2007, **50**, 5858.
12 W. L. Mock and N.-Y. Shih, *J. Org. Chem.*, 1986, **51**, 4440.
13 A. I. Day, A. P. Arnold, R. J. Blanch and B. Snushell, *J. Org. Chem.*, 2001, **66**, 8094.
14 C. Marquez, U. Pischel and W. M. Nau, *Org. Lett.*, 2003, **5**, 3911.
15 W. Ong, M. Gomez-Kaifer and A. E. Kaifer, *Org. Lett.*, 2002, **4**, 1791.
16 H. J. Kim, W. S. Jeon, Y. H. Ko and K. Kim, *Proc. Natl. Acad. Sci. U. S. A.*, 2002, **99**, 5007.
17 J. Lagona, P. Mukhopadhyay, S. Chakrabarti and L. Isaacs, *Angew. Chem., Int. Ed.*, 2005, **44**, 4844.
18 J. Kim, I.-S. Jung, S.-Y. Kim, E. Lee, J.-K. Kang, S. Sakamoto, K. Yamaguchi and K. Kim, *J. Am. Chem. Soc.*, 2000, **122**, 540.
19 Y.-M. Jeon, J. Kim, D. Wang and K. Kim, *J. Am. Chem. Soc.*, 1996, **118**, 9790.
20 N. J. Wheate, A. I. Day, R. J. Blanch, A. P. Arnold, C. Cullinane and J. G. Collins, *Chem. Commun.*, 2004, 1424.
21 M. S. Bali, D. P. Buck, A. J. Coe, A. I. Day and J. G. Collins, *Dalton Trans.*, 2006, 5337.
22 *HyperChem Release 7.5 for Windows Molecular Modelling System*, HyperCube Inc., Ontario, Canada, 2004.
23 D. T. Vistica, P. Skehan, D. Scudiero, A. Monks, A. Pittman and M. R. Boyd, *Cancer Res.*, 1991, **51**, 2515.
24 H.-Y. Fu, S.-F. Xue, Q.-J. Zhu, Z. Tao, J.-X. Zhang and A. I. Day, *J. Incl. Phenom. Macrocycl. Chem*, 2005, **52**, 101.
25 V. L. Bassini, D. Krieger, D. Duchene and D. Wouessidjewe, *J. Incl. Phenom. Mol. Recogn. Chem.*, 1996, **25**, 149.
26 C. Chassaing, M. Berger, A. Heckeroth, T. Ilg, M. Jaeger, C. Kern, K. Schmid and M. Uphoff, *J. Med. Chem.*, 2008, **51**, 1111.
27 H. Mizuuchi, V. Jaitely, S. Murdan and A. T. Florence, *Eur. J. Pharm. Sci.*, 2008, **33**, 326.
28 N. Saleh, A. L. Koner and W. M. Nau, *Angew. Chem., Int. Ed.*, 2008, **47**, 5398.
29 H. Jung, L. Medina, L. Garcia, I. Fuentes and R. Moreno-Esparaza, *J. Pharm. Pharmacol.*, 1998, **50**, 43.
30 Preliminary report from the Peter MacCullum Cancer Institute, Melbourne Australia.
31 S. E. Marriner, D. L. Morris, B. Dickson and J. A. Bogan, *Eur. J. Clin. Pharmacol.*, 1986, **30**, 705.